HEP'99 # 7_213
Submitted to Pa 7
Pl 7, 8

DELPHI 99-82 CONF 269
15 June 1999

Search for charginos and gravitinos at $\sqrt{s} = 189$ GeV

Preliminary

DELPHI Collaboration

Paper submitted to the HEP'99 Conference
Tampere, Finland, July 15-21

Search for charginos and gravitinos at $\sqrt{s} = 189$ GeV

Preliminary

DELPHI Collaboration

T.Alderweireld [1], **I.Gil** [2], **P.Rebecchi** [3]

Abstract

An update of the searches for charginos is presented, based on a data sample corresponding to the 158 pb^{-1} recorded by the DELPHI detector in 1998, at a centre-of-mass energy of 189 GeV. The search covers the case when the lightest neutralino is stable, as well as the case when it is unstable and decays into a photon and a gravitino. No evidence for a signal was found, new exclusion lower mass limits have been set.

[1] IISN, U. Mons Hainaut, Champ de Mars 7000 Mons, Belgium

[2] IFIC, Valencia-CSIC and DFAMN, U. de Valencia, E-46100 Burjassot (Valencia), Spain

[3] CERN, CH-1211 Geneva 23, Switzerland

1 Introduction

In 1998, the LEP centre-of-mass energy reached 189 GeV, and the DELPHI experiment collected an integrated luminosity of 158 pb^{-1}. These data have been analysed to search for the supersymmetric partners of Higgs and gauge bosons, the charginos, predicted by supersymmetric (SUSY) models [1].

A description of the parts of the DELPHI detector relevant to the present paper can be found in [2], while a complete description is given in [3].

The conservation of R-parity, implying a stable lightest supersymmetric particle (LSP), is assumed. So, in e^+e^- collisions charginos are pair produced. The Minimal Supersymmetric Standard Model (MSSM) scheme with universal parameters at the high mass scale typical of Grand Unified Theories (GUT's) is assumed [1]. The parameters of this model relevant to the present searches are the masses M_1 and M_2 of the gaugino sector (which are assumed to satisfy the GUT relation $M_1 = \frac{5}{3}\tan^2\theta_W M_2 \approx 0.5 M_2$ at the electroweak scale), the universal mass m_0 of the scalar lepton sector (which enters mainly via the sneutrino mass), the Higgs mass parameter μ, and the ratio $\tan\beta$ of the vacuum expectation values of the two Higgs doublets. As in Ref. [2] both cases where either the lightest neutralino ($\tilde{\chi}_1^0$) or the gravitino ($\tilde{\mathrm{G}}$) is the LSP are considered.

In the former case, the decay of the charginos is $\tilde{\chi}_1^{\pm}\to\tilde{\chi}_1^0 \mathrm{f}\bar{\mathrm{f}}'$ ($\mathrm{f}\bar{\mathrm{f}}'$ can be quarks or leptons) and the events are characterised by missing energy carried by the escaping $\tilde{\chi}_1^0$. In some areas of the parameter space, the charginos can decay to heavier neutralinos giving rise to a cascade effect: $\tilde{\chi}_1^{\pm}\to\tilde{\chi}_2^0 \mathrm{f}_1\bar{\mathrm{f}}_1'\to\tilde{\chi}_1^0\ \mathrm{f}_1\bar{\mathrm{f}}_1'\ \mathrm{f}_2\bar{\mathrm{f}}_2$ ($\mathrm{f}_1\bar{\mathrm{f}}_1'\ \mathrm{f}_2\bar{\mathrm{f}}_2$ can be quarks or leptons). The decay $\tilde{\chi}_2^0\to\tilde{\chi}_1^0\gamma$ may occur as well in some parameter regions. So the following decay channels were defined:

- The *leptonic* channel ($\ell\ell$): the decay products are only leptons and the LSPs.
- The *hadronic* channel (*jets*): the decay products are only quarks and the LSPs.
- The *semi-leptonic* channel ($jj\ell$): the decay products are quarks, leptons and the LSPs
- The *radiative* channel (*rad*): there is at least one isolated photon in the decay products.

In this scenario the likelihood ratio method is used to optimize the search for charginos [4]. An overview of this method and details of the implementation are given in 3.1.

In the latter case, the decay $\tilde{\chi}_1^0 \to \tilde{\mathrm{G}}\gamma$ is possible [5, 6, 7]. If the gravitino is sufficiently light (with a mass below about 10 eV/c^2 [7]), this decay takes place within the detector. As gravitinos escape detection, the typical signature of these SUSY events is missing energy and isolated photons. The same selection criteria used at centre-of-mass energy of 183 GeV are used in this scenario. The detailed description of the analysis can be found in Ref. [2].

2 Data samples and event generators

The total integrated luminosity collected by DELPHI during 1998 at $E_{cm} = 189$ GeV was 158 pb^{-1} and has been used for the present search.

To evaluate the signal efficiencies and background contaminations, events were generated using several different programs. All relied on JETSET 7.4 [8], tuned to LEP 1 data [9], for quark fragmentation.

The program SUSYGEN [10] was used to generate chargino production and decay events in both the neutralino LSP and the gravitino LSP scenarii, and to calculate masses, cross-sections and branching ratios for each adopted parameter sets. These agree with the calculations of Ref. [11]. Details of the signal samples generated are given in section 4.

The background process $e^+e^- \to q\bar{q}(n\gamma)$ was generated with PYTHIA 5.7 [8], while DYMU3 [12] and KORALZ 4.2 [13] were used for $\mu^+\mu^-(\gamma)$ and $\tau^+\tau^-(\gamma)$, respectively. The generator of Ref. [14] was used for $e^+e^- \to e^+e^-$ events. Processes leading to four-fermion final states, $(Z/\gamma)^*(Z/\gamma)^*$, W^+W^-, $We\nu_e$ and Ze^+e^-, were generated using EXCALIBUR [15] and GRC4F [16].

Two-photon interactions leading to hadronic final states were generated using TWOGAM [17], separating the VDM and QCD components. The generators of Berends, Daverveldt and Kleiss [18] were used for the QPM component and for leptonic final states.

The generated signal and background events were passed through the detailed simulation of the DELPHI detector [3] and then processed with the same reconstruction and analysis programs as the real data. The simulated number of events from different background processes was several times the number of the real data.

3 Event selections

The criteria used to select events were defined on the basis of the simulated signal and background events. The selections for charged and neutral particles were similar to those presented in [2], requiring charged particles to have momentum above 100 MeV/c and to extrapolate back to within 5 cm of the main vertex in the transverse plane, and to within twice this distance in the longitudinal direction. Calorimeter energy clusters above 100 MeV were taken as neutral particles if not associated to any charged particle track. The particle selection was followed by different event selections for the different signal topologies considered in the application of the likelihood ratio method.

3.1 The likelihood ratio method

The likelihood ratio method consists of combining several discriminating variables into one. This method, if the variables used are independent, gives the best possible background suppression for a given signal efficiency. The proof of this statement can be found in [4]. Consider a set of variables $\{x_n\}$, the probability density functions (pdf) of these variables are built by normalizing the distributions of these variables for the signal and the background. We denote the pdfs of these variables $f_i^S(x_i)$ for the signal events and $f_i^B(x_i)$ for the background events submitted to the same selection criteria. The likelihood ratio function is defined as $\mathcal{L}_\mathcal{R} = \prod_{i=1}^{n} \frac{f_i^S(x_i)}{f_i^B(x_i)}$. Events with $\mathcal{L}_\mathcal{R} > \mathcal{L}_{\mathcal{R}_{CUT}}$ are selected as candidate signal events. The value $\mathcal{L}_{\mathcal{R}_{CUT}}$ can be varied to select the desired purity or efficiency. The variables $\{x_n\}$ used to build the $\mathcal{L}_\mathcal{R}$ functions entering our analysis were chosen in the following set: the visible energy ($E_{\rm vis}$), visible mass ($M_{\rm vis}$), missing transversal momentum ($p_T^{\rm miss}$), polar angle of the missing momentum, number of charged particles, total number of particles, acoplanarity , acolinearity, ratio of electromagnetic energy to total

energy, percentage of total energy in a 30 degrees forward cone, kinematic information concerning the isolated photons, leptons and two most energetic charged particles and finally the jet informations. The optimal set of variables and the $\mathcal{L}_{\mathcal{RCUT}}$ were defined in order to have the minimal excluded cross-section at 95% of confidence level (C.L.) (see section 3.2).

3.2 Chargino analysis

The signal and background events were divided in four topologies : the leptonic topology ($\ell\ell_t$), the semi-leptonic topology ($jj\ell_t$), the hadronic topology ($jets_t$) and the radiative topology (rad_t) defined as :

- The $\ell\ell_t$ topology with no more than five charged tracks and no isolated photons.
- The $jj\ell_t$ topology with more than five charged tracks and at least one isolated lepton and no isolated photons.
- The $jets_t$ topology with more than five charged tracks and no isolated photons or leptons.
- The rad_t topology with at least one isolated photon.

The events in a given topology are mostly events of the corresponding decay channel, but events from other classes may also contribute. For instance, for low mass difference between the chargino and the LSP (low ΔM values, and thus visible energy) some events with hadronic decays are selected in the leptonic topology, and some semi-leptonic decay events with the isolated lepton unidentified are in the hadronic topology. This migration effect tends to disappear as ΔM increases. This effect is taken in to account in the final efficiency and limit computations.

The properties of the chargino decay products are mainly governed by the ΔM value. For low ΔM values, the signal events are similar to $\gamma\gamma$ events, for high ΔM to four fermions final states (W^+W^-, ZZ,..) while for intermediate ΔM values, the background is composed by all the SM processes in comparable proportions.

The simulated signal events were composed of 76 combinations of $\tilde{\chi}_1^\pm$ and $\tilde{\chi}_1^0$ masses for five chargino mass values ($M_{\tilde{\chi}_1^\pm} \approx 94$, 85, 70, 50 and 45 GeV/$c^2$) and with ΔM ranging from 1 GeV/c^2 to 70 GeV/c^2. A total of 152000 chargino events (2000 per combination) was generated and passed through the complete simulation of the DELPHI detector. The kinematic properties (acoplanarity, $E_{\rm vis}$, $p_T^{\rm miss}$,..) of the signal events were studied in terms of their mean value and standard deviation. Five ΔM regions were defined in order to have signal events with the same properties (table 1).

In these 20 windows (four topologies, five ΔM regions), a likelihood ratio function was defined. The generation of these 20 functions was performed in five steps:

- The signal distributions of all the variables used in this analysis (see section 3.1) were built with signal events generated with parameter sets giving rise to charginos and neutralinos with masses in the corresponding ΔM region. Only the events passing the corresponding ΔM topological cuts were used. The background distributions were built with background events passing the same ΔM topological cuts.

- Different preselection cuts were applied in these 20 windows in order to generate the probability density functions (pdfs). The pdfs were generated as mentioned in 3.1.

- Then, to reduce statistical fluctuations in the pdf distributions a smoothing was performed by passing the 20 sets of pdfs for signal and background through a triangular filter [19].

- In each window all the combinations of the pdfs were tested. Every combination defined a $\mathcal{L}_{\mathcal{R}}$ function (see section 3.1) and a $\mathcal{L}_{\mathcal{R}_{CUT}}$ computed in order to have the minimal excluded cross-section at 95% C.L. using the monochannel Bayesian formula [20]. The parameters entering this computation are the number of expected background events and the efficiency of the chargino selection. The efficiency of the chargino selection is defined in this case, as the number of events satisfying the $\mathcal{L}_{\mathcal{R}}$ divided by the total number of chargino events satisfying the topological preselection cuts.

- The combination of variables corresponding to the lowest excluded cross-section defined the $\mathcal{L}_{\mathcal{R}}$ function and the $\mathcal{L}_{\mathcal{R}_{CUT}}$ of this window. Finally, we chose the logical combination of the selections for different windows which gave the lowest excluded cross-section.

ΔM regions	
1	$5 \leq \Delta M < 10$ GeV/c^2
2	$10 \leq \Delta M < 25$ GeV/c^2
3	$25 \leq \Delta M < 35$ GeV/c^2
4	$35 \leq \Delta M < 50$ GeV/c^2
5	50 GeV/$c^2 \leq \Delta M$

Table 1: ΔM regions definition.

4 Results in case of a stable neutralino

4.1 Efficiencies and selected events

The total number of background events expected in the different topologies is shown in table 2, together with the number of events selected in the data.

The efficiencies of the chargino selection in the four topologies were computed separately for the 76 MSSM points using the $\mathcal{L}_{\mathcal{R}}$ function and the $\mathcal{L}_{\mathcal{R}_{CUT}}$ of the corresponding topology and ΔM region. To pass from the efficiencies of the chargino selection in the four topologies to the efficiencies in the four decay channels, all the migration effects were computed for all the generated points of the signal simulation. Then the efficiencies of the selection in the four decay channels were interpolated in the ($M_{\tilde{\chi}_1^\pm}$,$M_{\tilde{\chi}_1^0}$) plane using the method described in [2]. These efficiencies as function of $M_{\tilde{\chi}_1^\pm}$ and $M_{\tilde{\chi}_1^0}$ are shown in Fig. 1.

	Chargino channels (stable neutralino)				
	$5 \leq \Delta M < 10$ GeV/c^2				
Topology:	$jj\ell_t$	$jets_t$	$\ell\ell_t$	rad_t	TOTAL
Obs. events:	1	2	23	5	31
Background:	0.2 ± 0.95	1.8 ± 1.03	19.4 ± 1.15	3.4 ± 0.89	24.8 ± 2.02
	$10 \leq \Delta M < 25$ GeV/c^2				
Topology:	$jj\ell_t$	$jets_t$	$\ell\ell_t$	rad_t	TOTAL
Obs. events:	1	10	5	5	21
Background:	0.5 ± 0.95	6.9 ± 1.24	6.2 ± 1.13	3.4 ± 0.89	17.0 ± 2.12
	$25 \leq \Delta M < 35$ GeV/c^2				
Topology:	$jj\ell_t$	$jets_t$	$\ell\ell_t$	rad_t	TOTAL
Obs. events:	0	12	50	5	67
Background:	0.3 ± 0.93	10.4 ± 1.11	41.1 ± 1.55	3.4 ± 0.89	55.2 ± 2.30
	$35 \leq \Delta M < 50$ GeV/c^2				
Topology:	$jj\ell_t$	$jets_t$	$\ell\ell_t$	rad_t	TOTAL
Obs. events:	0	16	27	2	45
Background:	1.0 ± 0.93	17.0 ± 1.03	24.3 ± 1.11	1.7 ± 0.95	44.0 ± 2.02
	50 GeV/$c^2 \leq \Delta M$				
Topology:	$jj\ell_t$	$jets_t$	$\ell\ell_t$	rad_t	TOTAL
Obs. events:	1	78	43	2	124
Background:	1.3 ± 0.93	68.6 ± 1.25	43.8 ± 1.48	1.7 ± 0.95	115.4 ± 2.34

Table 2: The number of events observed in data and the expected number of background events in the different chargino search channels under the hypothesis of a stable neutralino (section 3.2).

All the selected events are compatible with the expectation from the background simulation. As no evidence for a signal is found, exclusion limits are set at 95% of C.L. using the multichannel Bayesian formula [20] taking in to account the branching ratio and the efficiency of each decay channel.

4.1.1 Limits

Limits on chargino production

The simulated data points were used to parametrise the efficiencies of the chargino selection criteria described in section 3.2 in terms of ΔM and the mass of the chargino (see section 4.1). Then a large number of SUSY points were investigated and the values of ΔM, the chargino and neutralino masses and the various decay branching ratios were determined for each point. By applying the appropriate efficiency (coming from the interpolation) and branching ratios and cross-sections for each channel decay (computed by SUSYGEN), the number of expected signal events for a given cross-section can be calculated. Taking in to account the expected background and the number of observed events, the corresponding point in the MSSM parameter space (μ, M_2, $\tan\beta$) can be excluded by requiring MSSM points to have a number of expected signal events greater than the upper limit at 95% C.L. on the number of observed events of the corresponding

ΔM region.

Fig.2 shows the chargino production cross-sections as obtained in the MSSM at $\sqrt{s} = 189$ GeV for different chargino masses for the non-degenerate ($\Delta M > 10$ GeV/c^2) and degenerate cases ($\Delta M = 5$ GeV/c^2) . The parameters M_2 and μ were varied randomly in the ranges 0 GeV/$c^2 < M_2 < 3000$ GeV/c^2 and –200 GeV/$c^2 < \mu < 200$ GeV/c^2 for three different values of $\tan\beta$, namely 1, 1.5 and 35. Two different cases were considered for the sneutrino mass: $M_{\tilde{\nu}} > 300$ GeV/c^2 (in the non degenerate case) and $M_{\tilde{\nu}} > 41$ GeV/c^2 (in the degenerate case).

To derive the chargino mass limits, constraints on the process $Z \rightarrow \tilde{\chi}_1^0\tilde{\chi}_2^0 \rightarrow \tilde{\chi}_1^0\tilde{\chi}_1^0\gamma$ were also included. These were derived from the DELPHI results on single-photon production at LEP 1 [21].

The chargino mass limits are summarized in Table 3. The table also gives, for each case, the minimal MSSM cross-section provided that $M_{\tilde{\chi}_1^\pm}$ is below the appropriate mass limit. These cross-section values are also displayed in Fig. 2. The minimal chargino mass limit versus ΔM, assuming a heavy sneutrino, is shown in Fig. 3.

In the non-degenerate case ($\Delta M > 10$ GeV/c^2) with a large sneutrino mass (> 300 GeV/c^2), the lower limit for the chargino ranges between 93.89 GeV/c^2 (for a mostly higgsino-like chargino) and 94.16 GeV/c^2 (for a mostly wino-like chargino). The minimal excluded MSSM cross-section at $\sqrt{s} = 189$ GeV is 0.24 pb, deriving from a chargino mass limit of 93.89 GeV/c^2. For $\Delta M > 20$ GeV/c^2, the lower limit for the chargino mass ranges between 94.12 GeV/c^2 and 94.23 GeV/c^2. The minimal excluded MSSM cross-section at $\sqrt{s} = 189$ GeV is in this case 0.14 pb.

In the degenerate case ($\Delta M = 5$ GeV/c^2), the cross-section does not depend significantly on the sneutrino mass, since the chargino is higgsino-like under the assumption of gaugino mass unification. The lower limit for the chargino mass, shown in Fig. 2, is 92.39 GeV/c^2. The lower cross section limit is in this case 0.69 pb.

A lower limit of 31.4 GeV/c^2 on the lightest neutralino mass is then obtained assuming $M_1/M_2 \geq 0.5$, using the obtained chargino exclusion regions and including DELPHI results [21] on the process $Z \rightarrow \tilde{\chi}_1^0\tilde{\chi}_2^0 \rightarrow \tilde{\chi}_1^0\tilde{\chi}_1^0\gamma$. The lowest mass limit is obtained for $\tan\beta = 1$, $\mu = -60.13$ GeV/c^2, $M_2 = 52.88$ GeV/c^2.

4.2 Results in case of an unstable neutralino

4.2.1 Efficiencies and selected events

The efficiency of the chargino selection for an unstable neutralino decaying into a photon and a gravitino was calculated from a total of 78000 events generated using the same combinations of $M_{\tilde{\chi}_1^\pm}$ and $M_{\tilde{\chi}_1^0}$ as in the stable neutralino scenario. As mentioned in [2], the same selection applies to all topologies. The efficiency, as shown in Fig. 4, varies only weakly with ΔM and is around 50%. Note that, due to the presence of the photons from the neutralino decay, the region of high degeneracy (down to $\Delta M = 1$ GeV/c^2) is fully covered.

The total number of background events expected in the different ΔM ranges is shown in table 4, together with the number of events selected in the data. 24 events were found in the data, with a total expected background of 19.9 $\pm$1.9. No signal was found and exclusion limits were set.

Case	$m_{\tilde{\nu}}$ (GeV/c^2)	$M_{\chi^{\pm}}^{min}$ (GeV/c^2)	σ^{max} (pb)	$\mathrm{N}_{95\%}$
Stable neutralino				
$\Delta M > 20$ GeV/c^2	> 300	94.12	0.14	11.1
$\Delta M > 10$ GeV/c^2	> 300	93.89	0.24	11.7
$\Delta M = 5$ GeV/c^2	> 41	92.39	0.69	12.3
Unstable neutralino				
$\Delta M > 10$ GeV/c^2	> 300	94.16	0.11	8.6
$\Delta M = 1$ GeV/c^2	> 41	94.21	0.08	7.1

Table 3: 95% confidence level limits for the chargino mass, the corresponding pair production cross-sections at 189 GeV and the 95% confidence level upper limit on number of observed events, for the non-degenerate and a highly degenerate cases. The scenarii of a stable $\tilde{\chi}_1^0$ and $\tilde{\chi}_1^0 \to \tilde{\mathrm{G}}\gamma$ are considered.

	Chargino channels (unstable neutralino)		
	Non-degenerate selection	Degenerate selection	Ultra-degenerate selection
Obs. events:	14	6	4
Background:	15.1 ± 1.3	2.6 ± 1.0	2.2 ± 1.0

Table 4: The number of events observed and the expected number of background events in the different ΔM cases under the hypothesis of an unstable neutralino (section 3.2).

4.2.2 Limits

The chargino cross-section limits corresponding to the case where the neutralino is unstable and decays via $\tilde{\chi}_1^0 \to \tilde{\mathrm{G}}\gamma$ are computed as explained in section 4.1.1 and they are shown in Fig.5 and in table 3. In the non-degenerate case the chargino mass limit at 95% C.L. is 94.16 GeV/c^2 for a heavy sneutrino, while in the ultra-degenerate case ($\Delta M = 1$ GeV/c^2) the limit is 94.21 GeV/c^2. The minimal MSSM cross-section excluded

by the above mass limits are 0.109 pb in the non degenerate case and 0.081 pb in the ultra-degenerate case.

5 Summary

Searches for charginos at $\sqrt{s} = 189$ GeV allow the exclusion of a large domain of SUSY parameters.

Assuming a difference in mass between chargino and neutralino, ΔM, of 10 GeV/c^2 or more, and a sneutrino heavier than 300 GeV/c^2, the existence of a chargino lighter than 93.89 GeV/c^2 can be excluded. If a gaugino-dominated chargino is assumed in addition, the kinematic limit is reached. If ΔM is 5 GeV/c^2, the lower limit on the chargino mass becomes 92.39 GeV/c^2, independent of the sneutrino mass.

A lower limit of 31.4 GeV/c^2 on the lightest neutralino mass is obtained assuming $M_1/M_2 \geq 0.5$, using the obtained chargino exclusion regions and including DELPHI results [21] on the process $\mathrm{Z} \to \tilde{\chi}_1^0\tilde{\chi}_2^0 \to \tilde{\chi}_1^0\tilde{\chi}_1^0\gamma$.

A specific $\tilde{\chi}_1^+\tilde{\chi}_1^-$ production search was performed assuming the decay of the lightest neutralino into photon and gravitino, giving somewhat more stringent limits on cross-sections and masses than in the case of a stable $\tilde{\chi}_1^0$.

References

[1] P. Fayet and S. Ferrara, Phys. Rep. **32** (1977) 249;
H.P. Nilles, Phys. Rep. **110** (1984) 1;
H.E. Haber and G.L. Kane, Phys. Rep. **117** (1985) 75.

[2] DELPHI Coll., P. Abreu *et al.*, Eur. Phys. J. **C1** (1998) 1-20.

[3] DELPHI Coll., P. Aarnio *et al.*, Nucl. Instr. and Meth. **303** (1991) 233;
DELPHI Coll., P. Abreu *et al.*, Nucl. Instr. and Meth. **378** (1996) 57.

[4] T.W. Anderson, An Introduction to multivariate analysis, New York Wiley, 1958.

[5] D. Dicus *et al.*, Phys. Rev. **D41** (1990) 2347;
D. Dicus *et al.*, Phys. Rev. **D43** (1991) 2951;
D. Dicus *et al.*, Phys. Lett. **B258** (1991) 231.

[6] S. Dimopoulos *et al.*, Phys. Rev. Lett. **76** (1996) 3494;
S. Ambrosanio *et al.*, Phys. Rev. Lett. **76** (1996) 3498;
J.L. Lopez and D.V. Nanopoulos, Mod. Phys. Lett. **A10** (1996) 2473;
J.L. Lopez and D.V. Nanopoulos, Phys. Rev. **D55** (1997) 4450.

[7] S. Ambrosanio *et al.*, Phys. Rev. **D54** (1996) 5395.

[8] T. Sjö strand, Comp. Phys. Comm. **39** (1986) 347;
T. Sjö strand, `PYTHIA 5.6` *and* `JETSET 7.3`, CERN-TH/6488-92.

[9] DELPHI Coll., P. Abreu *et al.*, Z. Phys. **C73** (1996) 11.

[10] S. Katsanevas and S. Melachroinos in *Physics at LEP2*, CERN 96-01, Vol. 2, p. 328.

[11] S. Ambrosanio and B. Mele, Phys. Rev. **D52** (1995) 3900;
S. Ambrosanio and B. Mele, Phys. Rev. **D53** (1996) 2451.

[12] J.E. Campagne and R. Zitoun, Z. Phys. **C43** (1989) 469.

[13] S. Jadach, B.F.L. Ward and Z. Was, Comp. Phys. Comm. **79** (1994) 503.

[14] F.A. Berends, R. Kleiss, W. Hollik, Nucl. Phys. **B304** (1988) 712.

[15] F.A. Berends, R. Pittau, R. Kleiss, Comp. Phys. Comm. **85** (1995) 437.

[16] J.Fujimoto *et al.*, Comp. Phys. Comm. **100** (1997) 128

[17] S. Nova, A. Olshevski, and T. Todorov, *A Monte Carlo event generator for two photon physics*, DELPHI note 90-35 (1990).

[18] F.A. Berends, P.H. Daverveldt, R. Kleiss, Comp. Phys. Comm. **40** (1986) 271, Comp. Phys. Comm. **40** (1986) 285, Comp. Phys. Comm. **40** (1986) 309.

[19] A.V. Oppenheim and R.W. Schafer, Discrete-time signal processing, Prentice-Hall, 1989

[20] V.F. Obraztsov, Nucl. Instr. and Meth. **316** (1992) 388;
V.F. Obraztsov, Nucl. Instr. and Meth. **399** (1997) 500.

[21] DELPHI Coll., P. Abreu *et al.*, Z. Phys. **C74** (1997) 577

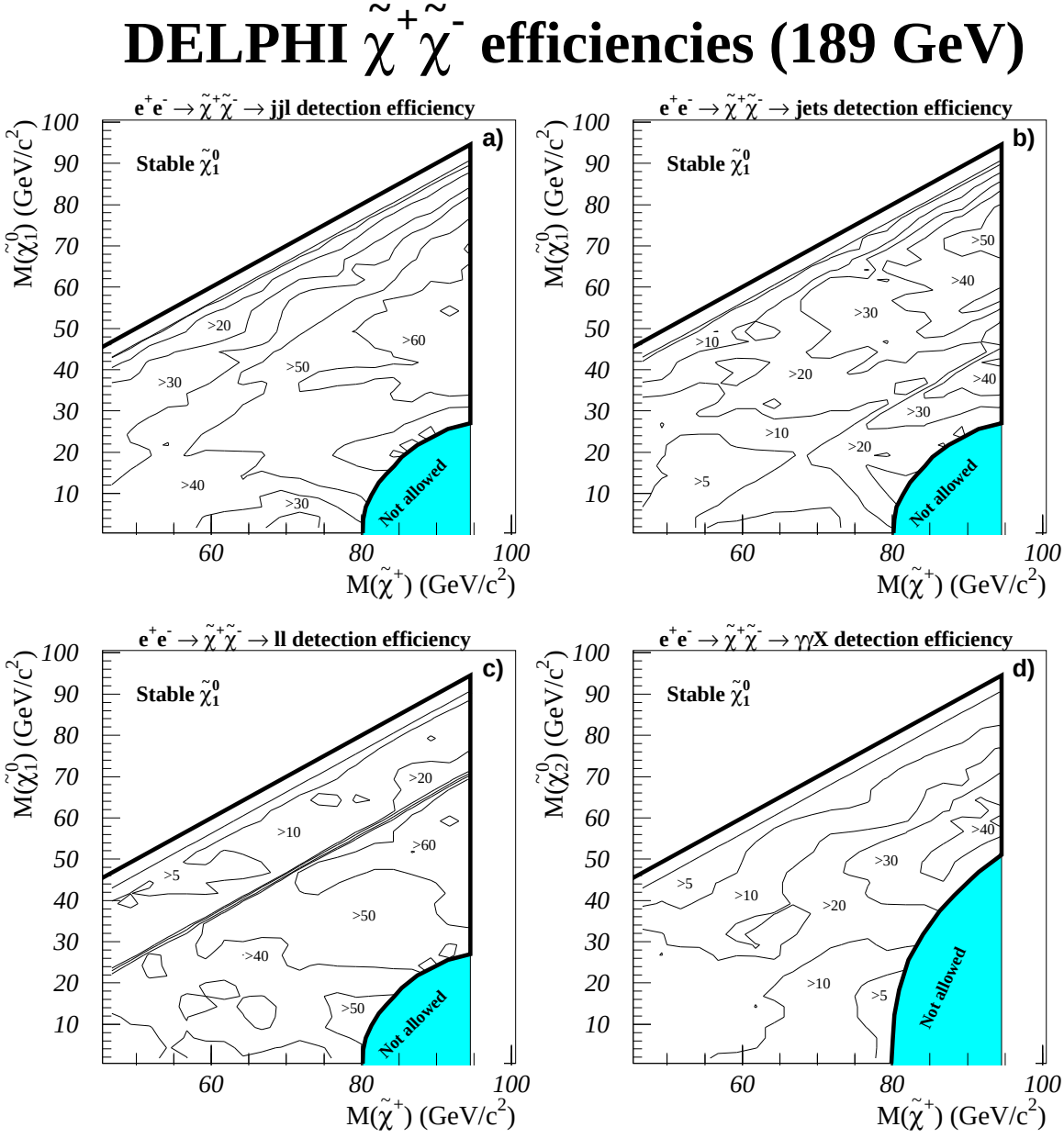

Figure 1: Chargino detection efficiencies (stable neutralino) for the 4 channels decay a) $jj\ell$, b) *jets*, c) $\ell\ell$ and d) *rad*, obtained from the parametrisation described in section 3.2.

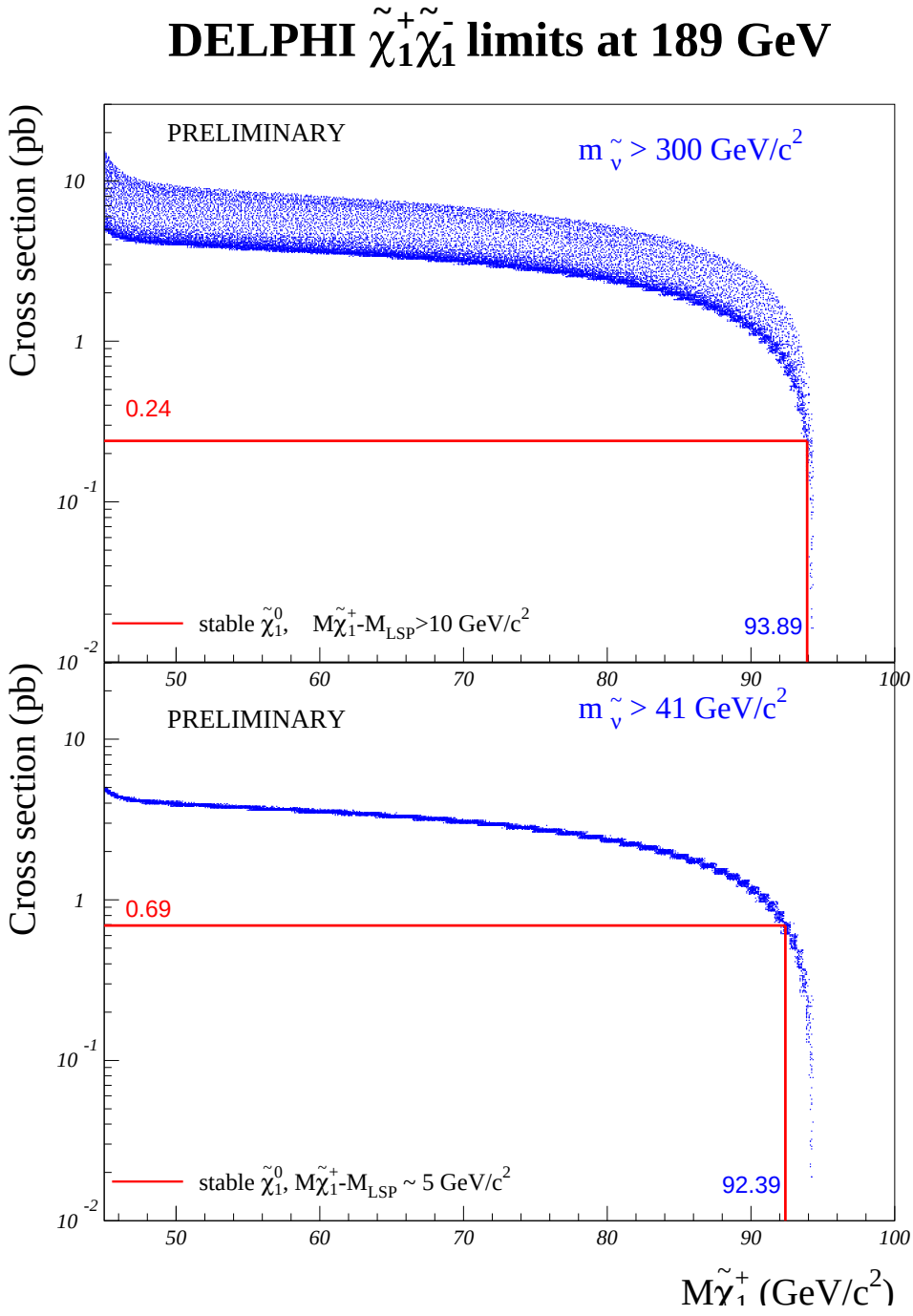

Figure 2: Expected cross-sections at 189 GeV (dots) versus the chargino mass in the non-degenerate scenario ($\Delta M > 10$ GeV/c^2) and in the degenerate scenario ($\Delta M \sim 5$ GeV/c^2), for different MSSM parameter values, in the case of stable neutralino. A heavy sneutrino ($m_{\tilde{\nu}} > 300$ GeV/c^2) has been assumed in the upper plot and $m_{\tilde{\nu}} > 41$ GeV/c^2 in the lower one. The indicated cross-sections are the minimal ones in the excluded mass region.

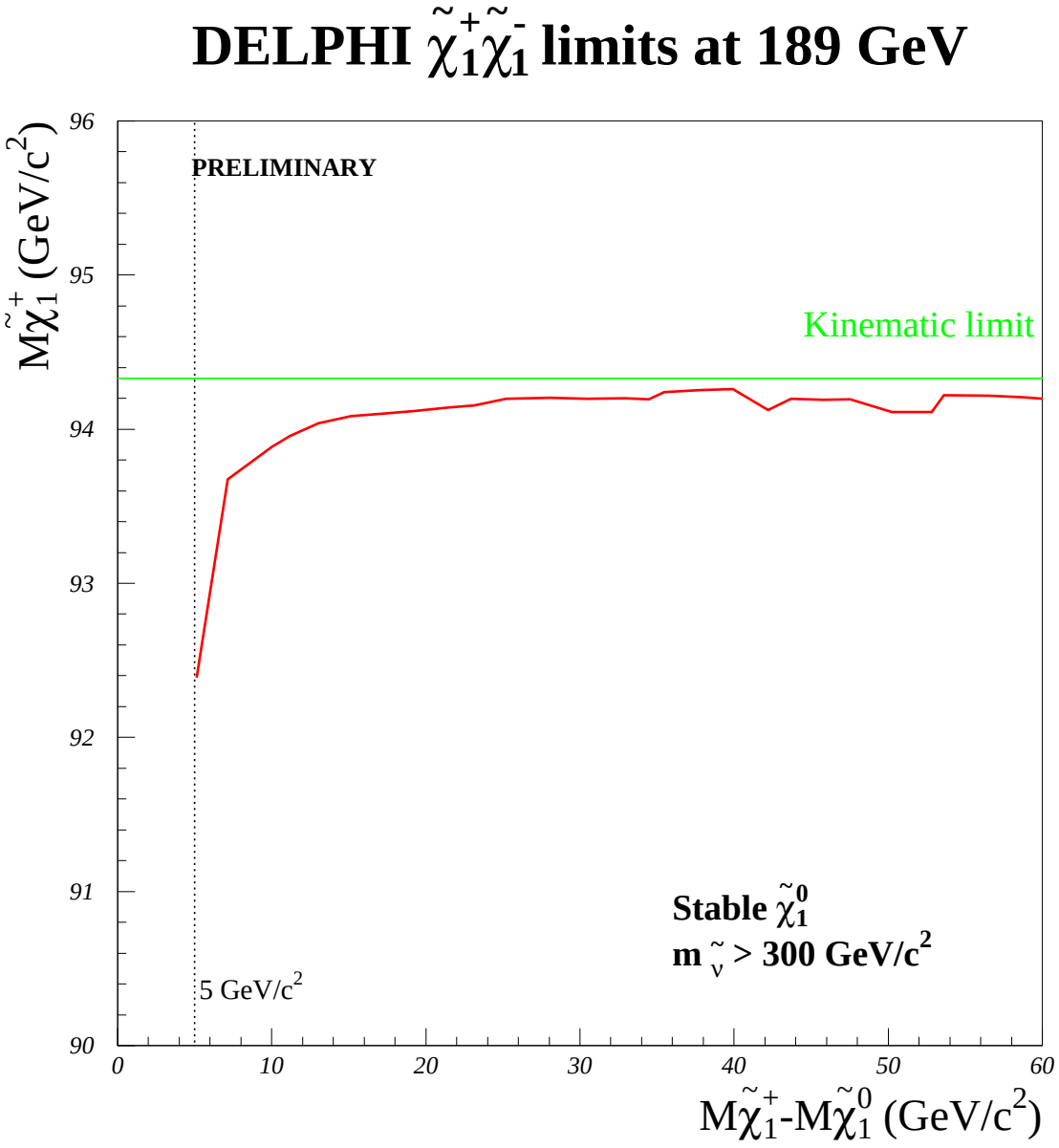

Figure 3: The chargino mass limit as function of the ΔM value under the assumption of a heavy sneutrino. The straight horizontal line shows the kinematic limit in the production and the decay. The limit applies in the case of a stable neutralino.

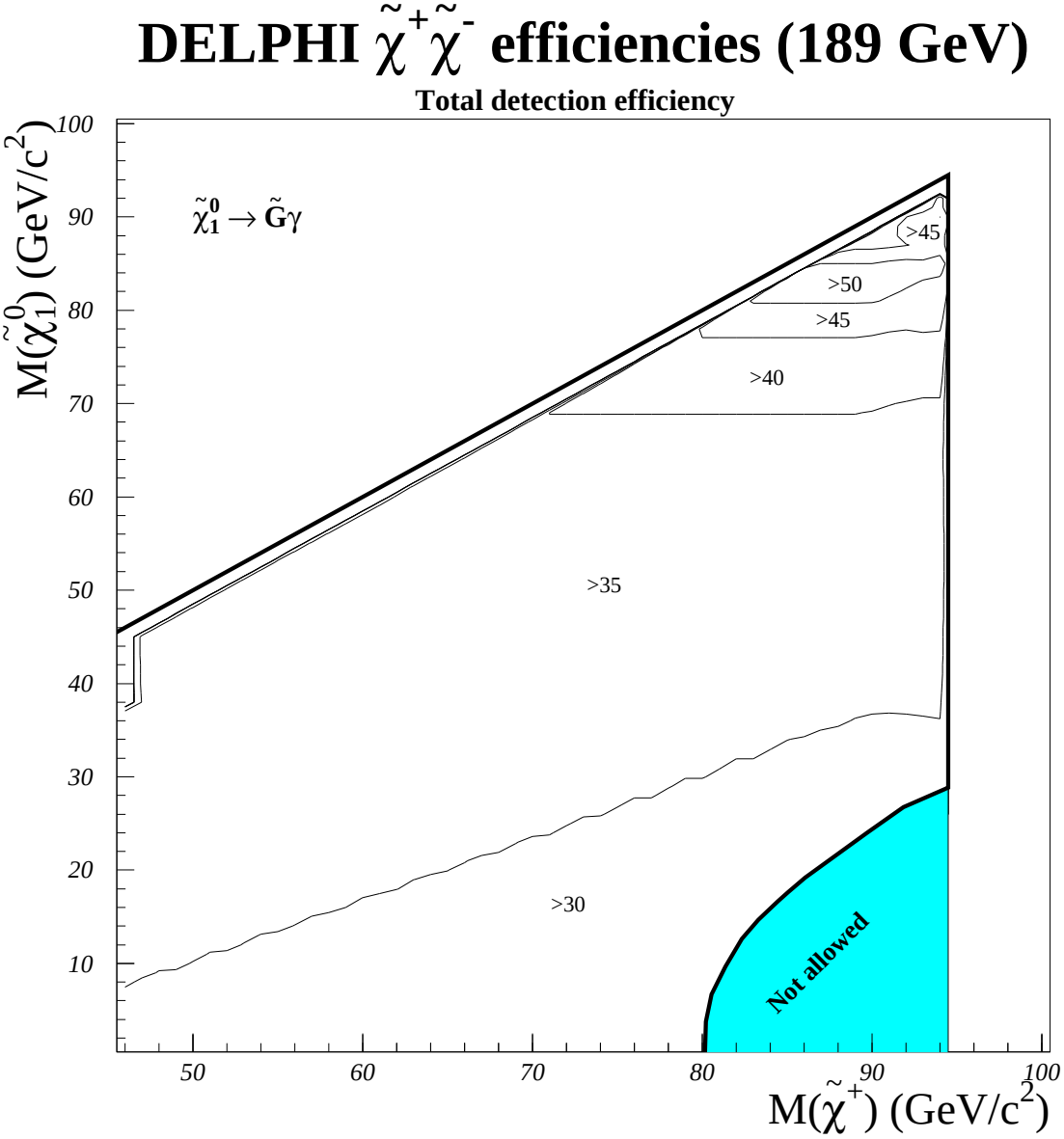

Figure 4: Chargino detection efficiencies in case of unstable neutralino.

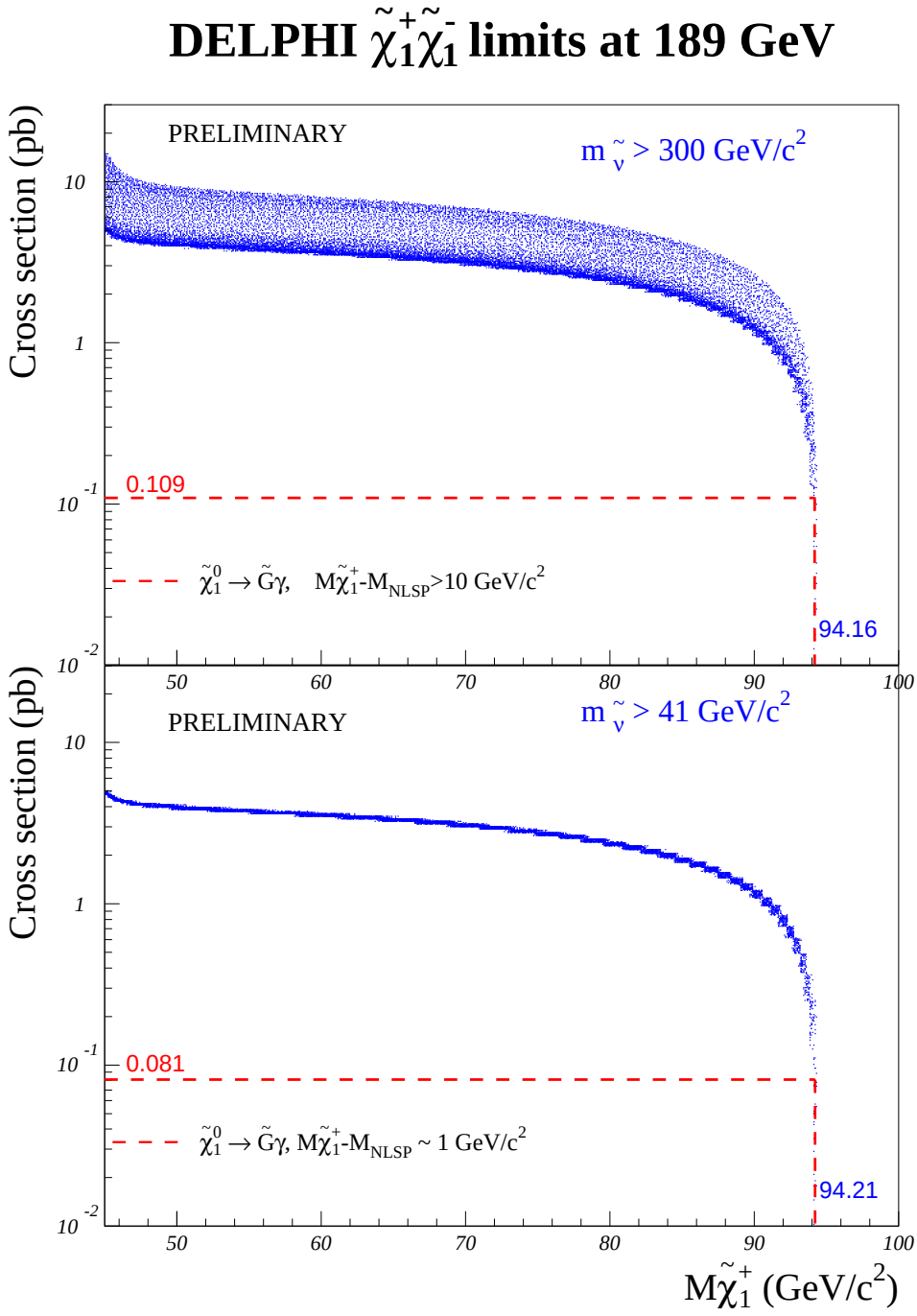

Figure 5: Expected cross-sections at 189 GeV (dots) versus the chargino mass in the non-degenerate scenario ($\Delta M > 10$ GeV/c^2) and in the ultra-degenerate scenario ($\Delta M \sim 1$ GeV/c^2), for different MSSM parameter values, in the case of unstable neutralino. A heavy sneutrino ($m_{\tilde{\nu}} > 300$ GeV/c^2) has been assumed in the upper plot and $m_{\tilde{\nu}} > 41$ GeV/c^2 in the lower one. The indicated cross-sections are the minimal ones in the excluded mass region.